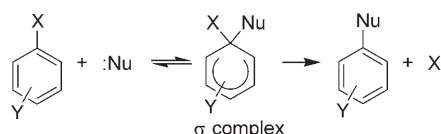


# Observation of an Isolated Intermediate of the Nucleophilic Aromatic Substitution Reaction by Infrared Spectroscopy\*\*

Hayato Hasegawa, Kenta Mizuse, Masaki Hachiya, Yoshiyuki Matsuda, Naohiko Mikami, and Asuka Fujii\*

Nucleophilic aromatic substitution (Scheme 1) is a major reaction of electron-deficient aromatic compounds.  $\sigma$  Complexes are generally presumed to play the role of the intermediate or the transition state in this reaction,<sup>[1,2]</sup> and it is, therefore, important to understand the structures and inherent stability of the  $\sigma$  complexes.



**Scheme 1.** General mechanism of the nucleophilic substitution reaction. X = leaving group, Y = electron-withdrawing group, Nu = nucleophile.

Extensive studies have shown that nucleophilic aromatic substitution reactions occur upon ionization of the gas-phase clusters formed from halogen-substituted benzene and polar solvent molecules.<sup>[3–10]</sup> In such systems, ionization causes the aromatic compounds to become highly electron deficient, thus ensuring the high reaction efficiencies. Recently, several  $\sigma$ -complex-type structures, such as  $\text{H}^+\text{C}_6\text{H}_6$ ,  $\text{H}^+\text{C}_6\text{H}_5\text{F}$ ,  $(\text{C}_6\text{H}_6\text{-NH}_3)^+$ , and  $[\text{CH}_3\text{OC}_6\text{H}_3(\text{NO}_2)_3]^+$  have been observed in the gas phase by spectroscopy.<sup>[11–15]</sup> However, the elimination step is unfavorable in these cases because of their poor leaving group ( $\text{X} = \text{H}$ ). As a result, the high yields of the  $\sigma$  complexes sacrificed their ability to act as reaction intermediates. Such intermediate structures have not so far been reported for systems in which the substitution reactions can actually occur.

Intracluster substitution reactions have only been observed in the cases of halobenzenes. The cluster cations formed from hexafluorobenzene ( $\text{C}_6\text{F}_6$ ) and polar molecules are very attractive targets to probe the intermediate structures in the reaction because there are no *ortho/meta/para* isomers and only one type of structure for the  $\sigma$  complex is expected.

In this study, we report the first experimental observation of a stable  $\sigma$  complex for a system in which aromatic substitution actually occurs. We employed the efficient direct ionization of  $\text{C}_6\text{F}_6$  by coherent vacuum ultraviolet (VUV) light,<sup>[16]</sup> and confirmed the high substitution reactivity of the  $\text{C}_6\text{F}_6^+/\text{NH}_3$  system to produce  $\text{C}_6\text{F}_5\text{NH}_2^+$ . We also measured the infrared spectrum of the  $(\text{C}_6\text{F}_6\text{-NH}_3)^+$  cluster cation and showed that the cluster cation forms an intermediate  $\sigma$  complex.

Figure 1 shows the mass spectrum of the ions produced by the one-photon ionization of the  $\text{C}_6\text{F}_6/\text{NH}_3/\text{He}$  mixture by VUV light. The most intense signal at  $m/z$  186 corresponds to  $\text{C}_6\text{F}_6^+$ . The signal at  $m/z$  183 is uniquely assigned to the substitution reaction product  $\text{C}_6\text{F}_5\text{NH}_2^+$ . The intensity of this signal is comparable to that of  $\text{C}_6\text{F}_6^+$ , and it clearly demonstrates that, upon ionization, the reaction efficiently proceeds in the  $\text{C}_6\text{F}_6/\text{NH}_3$  system with the elimination of HF.

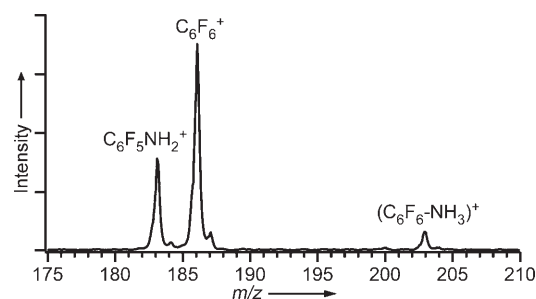


**Figure 1.** Mass spectrum of the ions produced by the one-photon ionization of the  $\text{C}_6\text{F}_6/\text{NH}_3$  mixture with VUV light.

The signal at  $m/z$  203 is attributed to the  $(\text{C}_6\text{F}_6\text{-NH}_3)^+$  cluster cation. The IR spectrum of the cluster cation is shown in Figure 2a. When this spectrum was measured, the mass resolution of the second quadrupole mass spectrometer was reduced to  $\Delta m \approx 10$  to give sufficient fragment intensity, and either or both the  $\text{C}_6\text{F}_6^+$  and  $\text{C}_6\text{F}_5\text{NH}_2^+$  fragment ions were monitored when recording the spectrum. Three bands are seen in the NH stretching region of the IR spectrum, with the two bands at the higher frequencies nearly degenerate. These three bands clearly result from the symmetric and degener-

[\*] H. Hasegawa, K. Mizuse, M. Hachiya, Dr. Y. Matsuda, Prof. N. Mikami, Prof. A. Fujii  
Department of Chemistry  
Graduate School of Science  
Tohoku University  
Sendai 980-8578 (Japan)  
Fax: (+81) 22-795-6785  
E-mail: asukafujii@mail.tains.tohoku.ac.jp  
Homepage: <http://www.mikamilab.chem.tohoku.ac.jp>

[\*\*] We are grateful to Dr. Toshihiko Maeyama for helpful discussions. This study was supported by a Grant-in-Aid for Scientific Research (Japan): Project No. 19056001 from MEXT and Nos. 19205001, 20550005, 20750002, and 20-5015 from the JSPS. K.M. is supported by JSPS Research Fellowships for Young Scientists. Most of the calculations were performed at the Research Center for Computational Science, Okazaki (Japan).

Supporting information for this article is available on the WWW under <http://dx.doi.org/10.1002/ange.200801751>.

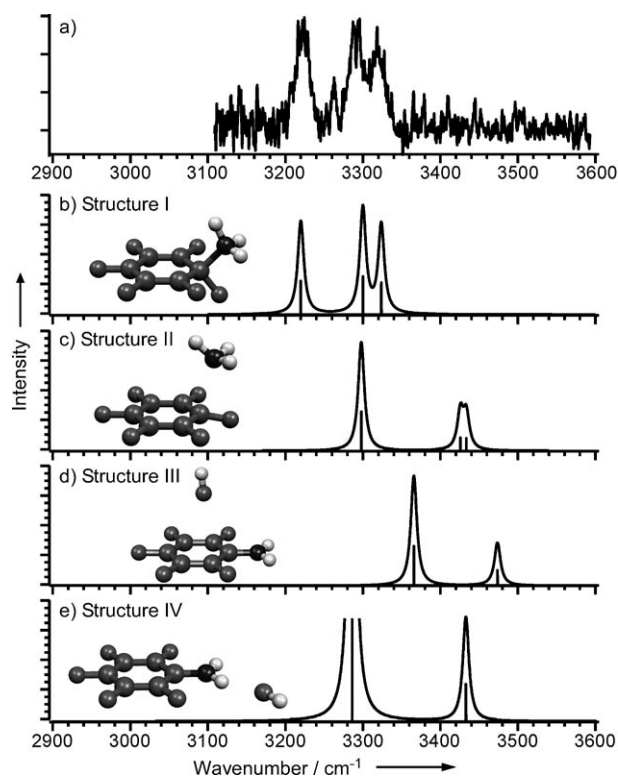


**Figure 2.** Observed and simulated infrared spectra of the  $(\text{C}_6\text{F}_6\text{-NH}_3)^+$  complex. a) Observed spectrum obtained by monitoring either the  $\text{C}_6\text{F}_6^+$  and/or  $\text{C}_6\text{F}_5\text{NH}_2^+$  fragments. b)–e) Simulated spectra obtained with B3LYP/6-311 + G(2df,2pd) and a scale factor of 0.953. The stick spectra in the simulations were transformed into the continuous spectra by using Lorentzian functions with a full-width at half-maximum value of  $10\text{ cm}^{-1}$ .

ated asymmetric NH stretching bands of the ammonia moiety, and the small splitting of the asymmetric bands suggests that the effective symmetry of the ammonia moiety is lower than  $\text{C}_3$  in the cluster cation.

To identify the geometrical structure of  $(\text{C}_6\text{F}_6\text{-NH}_3)^+$ , we carried out density functional theory calculations at the B3LYP/6-311 + G(2df,2pd) level. Four stable structures were found after energy optimization, and simulation of their IR spectra, on the basis of the harmonic frequencies scaled by a factor of 0.953, are shown in Figure 2b–e. Structure I is a  $\sigma$  complex. The internuclear distance between the N atom of the ammonia moiety and the C atom of the phenyl ring is only  $1.57\text{ \AA}$ , and a covalent bond is clearly formed between these two moieties. In addition, the C–F bond length of the leaving position ( $1.38\text{ \AA}$ ) is longer than the other C–F bonds ( $1.30$ – $1.33\text{ \AA}$ ). Structures II to IV correspond to the minima in the entrance and exit channels of the substitution reaction. In structure II, the  $\text{C}\cdots\text{N}$  distance is  $2.46\text{ \AA}$ , and it can be regarded as a cluster held together through charge–dipole interactions. The substitution reaction has been completed in structures III and IV, and the escaping HF fragment is trapped by the charge–dipole interaction and/or the hydrogen bond. As the substitution reaction is highly exothermic, structure IV is the most stable isomer, as shown in the energy diagram (Figure 3).

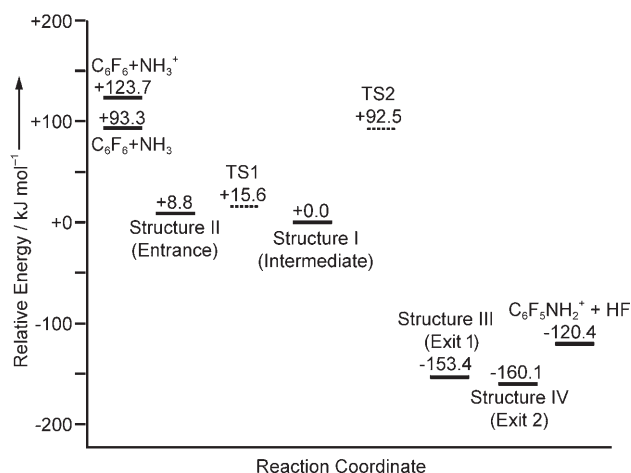


**Figure 3.** Calculated energy diagram of the nucleophilic aromatic substitution reaction occurring in the  $(\text{C}_6\text{F}_6\text{-NH}_3)^+$  system. Calculations were carried out at the ROMP2/6-311 + G(2df,2pd)//B3LYP/6-311 + G(2df,2pd) level. Zero-point corrections are included in the presented energy values. Each of the transition states is the calculated maximum in the relaxed potential-energy surface; see the Experimental Section and Supporting Information.

Comparison of the observed and simulated IR spectra clearly demonstrates that only structure I reproduces the observed IR spectra. As the new C–N covalent bond in structure I is formed by the donation of the lone pair electrons from the ammonia moiety to the hole in the  $\pi$  orbital, the NH stretching frequencies show low-frequency shifts relative to those of structure II. The greater intermolecular interaction in structure I also clearly lifts the degeneracy in the asymmetric NH stretching bands. The simulations of structures III and IV show only two NH stretching bands because the ammonia moiety is transformed into the amino group by elimination of HF. From the IR simulations, the observed IR spectrum clearly demonstrates that  $(\text{C}_6\text{F}_6\text{-NH}_3)^+$  is the intermediate structure in the nucleophilic aromatic substitution reaction.

The energy diagram of the nucleophilic substitution reaction calculated at the ROMP2/6-311 + G(2df,2pd)//B3LYP/6-311 + G(2df,2pd) level is shown in Figure 3. Transition states TS1 and TS2 are the maxima in the relaxed potential-energy surface (PES). TS1 lies just above structure II, which shows that structure II is almost metastable. Furthermore, structures III and IV are close to the exit of the reaction channel, and therefore, their dissociation energies are much lower than the energy of the reaction intermediate, structure I. Therefore, once the system goes over the energy barrier from structure I to III or IV, the system cannot be trapped at either structure III or IV, and dissociates into the products. These are the reasons for the absence of a contribution of structures II to IV to the observed IR spectrum. The IR photon energy (typically  $40\text{ kJ mol}^{-1}$ ) is smaller than both the dissociation energy of structure I ( $93.3\text{ kJ mol}^{-1}$ ) and the height of the reaction barrier (TS2,  $92.5\text{ kJ mol}^{-1}$ ). This fact means that a multi-photon process or high internal energies are required to observe the intermediate by photodissociation spectroscopy.

In conclusion, the experimental IR spectrum of  $(\text{C}_6\text{F}_6\text{-NH}_3)^+$  demonstrates that the cluster cation forms a  $\sigma$  complex. This is the first identification of a stable intermediate in a nucleophilic aromatic substitution reaction that occurs efficiently in the cationic state.

## Experimental Section

The experimental apparatus has been described elsewhere,<sup>[17,18]</sup> and only a brief description is given here. Resonance-enhanced multiphoton ionization is very inefficient for  $\text{C}_6\text{F}_6$  because of its fast internal conversion in its excited states.<sup>[19]</sup> Therefore, a coherent VUV light (118 nm) was employed to ionize  $\text{C}_6\text{F}_6$ . The VUV light was generated by tripling the third harmonics of a YAG laser output with a Xe/Ar gaseous mixture. The  $\text{C}_6\text{F}_6/\text{NH}_3/\text{He}$  mixture was jet-expanded into a vacuum chamber, which was equipped with a tandem-type quadrupole mass spectrometer connected by an octapole ion guide.  $\text{C}_6\text{F}_6$  was ionized by the light (wavelength 118 nm) in the collisional region of the jet-expansion, and cluster ions of  $\text{C}_6\text{F}_6$  and  $\text{NH}_3$  were produced by collisional cooling. The 1:1 cluster cation was uniquely mass-selected by the first quadrupole mass spectrometer, and was irradiated by IR light in the  $3\text{ }\mu\text{m}$  region with an optical parametric oscillator. The dissociation fragment arising from the IR vibrational excitation was mass-selected by the second mass spectrometer. The IR spectrum of the 1:1 cluster was measured by scanning the IR wavelengths while monitoring the fragment intensity.

For a detailed analysis of the observed spectrum and cluster structure, quantum chemical calculations were carried out. Geometry optimizations were carried out by density functional theory calculations with the B3LYP functional and the 6-31 + G(d) basis set for the initial explorations, and with the larger 6-311 + G(2df,2pd) basis set for the final optimizations. These geometries were used for further calculations. Harmonic frequencies and IR intensities were calculated at the B3LYP/6-311 + G(2df,2pd) level and the calculated frequencies were scaled by a single factor of 0.953. The energy diagram in Figure 3 was obtained from the relaxed potential-energy surface (PES) scan. One of the parameters, the C...N distance for the entrance channel or the H...F distance for the exit channel, was scanned while optimizing all the other parameters at the B3LYP/6-311 + G(2df,2pd) level. The stabilization energies at all the optimized points were recalculated at the ROMP2/6-311 + G(2df,2pd) level. The values in Figure 3 include the zero-point energy (ZPE) corrections at the DFT calculations, in which the ZPE correction terms were also scaled by the factor of 0.953. A plot of the PES is shown in the Supporting Information (Figure S1). Further calculations, such as the intrinsic reaction coordinate (IRC) calculation, have not been done because of the limitation of the ROMP2 calculation. All the calculations in this study were carried out using the Gaussian 03 program, and the cluster structures are drawn with the MOLEKEL program.<sup>[20]</sup> Optimized

geometries and absolute energies of the four isomers are shown in the Supporting Information.

Received: April 15, 2008

Published online: July 9, 2008

**Keywords:** aromatic substitution · gas-phase reactions · ion-molecule reactions · IR spectroscopy · reaction intermediates

- [1] G. W. Wheland, *J. Am. Chem. Soc.* **1942**, *64*, 900–908.
- [2] F. Terrier, *Chem. Rev.* **1982**, *82*, 77–152.
- [3] O. Dimopoulou-Rademann, K. Rademann, P. Bisling, B. Brutschy, *Ber. Bunsen-Ges.* **1984**, *88*, 215–217.
- [4] T. Maeyama, N. Mikami, *J. Am. Chem. Soc.* **1988**, *110*, 7238–7239.
- [5] B. Brutschy, C. Janes, J. Eggert, *Ber. Bunsen-Ges.* **1988**, *92*, 435–437.
- [6] D. Thölmann, H. F. Grützmaier, *J. Am. Chem. Soc.* **1991**, *113*, 3281–3287.
- [7] B. Brutschy, *Chem. Rev.* **1992**, *92*, 1567–1587.
- [8] H. F. Grützmaier, *Org. Mass Spectrom.* **1993**, *28*, 1375–1387.
- [9] C. Dedonder-Lardeux, I. Dimicoli, C. Jouvet, S. Martrenchard-Barra, M. Richard-Viard, D. Solgadi, M. Vervloet, *Chem. Phys. Lett.* **1995**, *240*, 97–140.
- [10] H. Tachikawa, *J. Phys. Chem. A* **2006**, *110*, 153–159.
- [11] N. Solcà, O. Dopfer, *Angew. Chem.* **2002**, *114*, 3781–3784; *Angew. Chem. Int. Ed.* **2002**, *41*, 3628–3631.
- [12] N. Solcà, O. Dopfer, *J. Am. Chem. Soc.* **2003**, *125*, 1421–1430.
- [13] O. Dopfer, *J. Phys. Org. Chem.* **2006**, *19*, 540–551.
- [14] K. Mizuse, A. Fujii, N. Mikami, *J. Phys. Chem. A* **2006**, *110*, 6387–6390.
- [15] B. Chiavarino, M. E. Crestoni, S. Fornarini, F. Lanucara, J. Lemaire, P. Maitre, *Angew. Chem.* **2007**, *119*, 2041–2044; *Angew. Chem. Int. Ed.* **2007**, *46*, 1995–1998.
- [16] As the photon energy of the VUV light of wavelength 118 nm (10.48 eV) is higher than the vertical ionization energies of both  $\text{C}_6\text{F}_6$  (9.90 eV) and  $\text{NH}_3$  (10.07 eV), it is also possible that the  $\text{NH}_3^+$  precursor ion reacts with  $\text{C}_6\text{F}_6$  to produce the  $(\text{C}_6\text{F}_6\text{-NH}_3)^+$  species.
- [17] M. Miyazaki, A. Fujii, T. Ebata, N. Mikami, *Phys. Chem. Chem. Phys.* **2003**, *5*, 1137–1148.
- [18] Y. Matsuda, M. Mori, M. Hachiya, A. Fujii, N. Mikami, *Chem. Phys. Lett.* **2006**, *422*, 378–381.
- [19] M. Z. Zgierski, T. Fujiwara, E. C. Lim, *J. Chem. Phys.* **2005**, *122*, 144312.
- [20] a) Gaussian 03 (Revision D.01), M. J. Frisch et al., see the Supporting Information; b) MOLEKEL 4.3, P. Flukiger, H. P. Luthi, S. Portmann, J. Weber, Swiss Center for Scientific Computing, Manno (Switzerland), **2000–2002**.